

${}^3,{}^4\text{He}(\bar{p},\pi^+){}^4,{}^5\text{He}_{g.s.}$  reactions at 800 MeV

B. Höistad

*University of Texas at Austin, Austin, Texas 78712*

M. Gazzaly

*University of Minnesota, Minneapolis, Minnesota 55455*

B. Aas, G. Igo, A. Rahbar, and C. Whitten

*University of California, Los Angeles, California 90024*

G. S. Adams

*University of South Carolina, Columbia, South Carolina 29208*

R. Whitney

*University of Virginia, Charlottesville, Virginia 22903*

(Received 12 September 1983)

Angular distributions of the differential cross section and the analyzing power for ground state transitions in the  ${}^3,{}^4\text{He}(\bar{p},\pi^+){}^4,{}^5\text{He}$  reactions have been measured at 800 MeV using a polarized proton beam. The angular distributions of the analyzing power  $A_y$  reveal a surprisingly strong spin dependence in these reactions. The analyzing power from the  ${}^3\text{He}(\bar{p},\pi^+){}^4\text{He}$  reaction is compared with  $A_y$  data from elastic p-He scattering, the  $pp\rightarrow d\pi$  reaction, and pion nucleon scattering, in order to find an indication of the origin to the spin dependence. Reasonably good agreement is obtained with the pion-nucleon  $A_y$  data when momentum sharing is assumed between the nuclear vertices involved in a pion rescattering diagram of the  $(p,\pi)$  reaction.

$$\left[ \begin{array}{l} \text{NUCLEAR REACTIONS } {}^3\text{He}(\bar{p},\pi^+){}^4\text{He}, {}^4\text{He}(\bar{p},\pi^+){}^5\text{He}, E_x=0 \text{ MeV,} \\ T_p=800 \text{ MeV; measured } \sigma(E,\theta), A_y \text{ from } \theta_{c.m.}^{\text{m}}=10^\circ \text{ to } 80^\circ. \text{ Comparisons with} \\ A_y \text{ from } {}^3,{}^4\text{He}(\bar{p},p){}^3,{}^4\text{He}, \bar{p}p\rightarrow d\pi, \text{ and } \pi\bar{p}. \end{array} \right]$$

## I. INTRODUCTION

The  $(p,\pi)$  reaction on nuclei has been extensively studied at energies near the production threshold.<sup>1</sup> The experimental data base now includes differential cross sections as well as analyzing powers from numerous nuclear transitions, for both positive and negative pion production. From these studies it is apparent that the  $(p,\pi)$  reaction is very sensitive to the nuclear structure. However, it is still unclear how a successful theoretical calculation should be performed, although the basic ingredients in the reaction mechanism are believed to be known. Different schemes for treating the crucial pion rescattering in the process have had partial success,<sup>1</sup> but a truly convincing case where several experimental parameters are well predicted is still missing. A particularly troublesome problem in the interpretation of the reaction has been to comprehend the interplay between the reaction mechanism and the nuclear structure.

The high energy behavior of the  $(p,\pi)$  reaction is not very well known. Preliminary data between 600 and 800 MeV indicate a weaker nuclear structure dependence than the threshold data, at least as reflected in the angular distributions of the differential cross section.<sup>1</sup> However, preliminary data on the analyzing power for the  ${}^2\text{H}(\bar{p},\pi^+){}^3\text{H}$  reaction<sup>2</sup> indicate that there might be a substantial spin

dependence in the  $(p,\pi)$  reaction in this energy region. If this spin dependence is connected to the reaction mechanism rather than to simple initial and final state interaction, the analyzing power data should be most important, in order to enable a better understanding of the reaction mechanism at these energies.

In the following we present the first measurements of the  $(\bar{p},\pi^+)$  analyzing power at 800 MeV from target nuclei with  $A > 2$ . Angular distributions of the differential cross section and the analyzing power from the ground state transitions in the  ${}^3\text{He}(\bar{p},\pi^+){}^4\text{He}$  and  ${}^4\text{He}(\bar{p},\pi^+){}^5\text{He}$  reactions have been measured in the angular range  $\theta_{c.m.}=5^\circ-85^\circ$ . A phenomenological comparison is made with data from different plausible subprocesses in the  $(\bar{p},\pi)$  reaction, namely, the  $\bar{p}p\rightarrow\pi d$  reaction and elastic pion-nucleon scattering. The proton distortion is also discussed as a possible source of the spin dependence in the  $(\bar{p},\pi^+)$  reaction.

## II. EXPERIMENTAL DETAILS

This experiment was performed with the 800 MeV polarized proton beam from the Clinton P. Anderson Meson Physics Facility (LAMPF), using the high resolution spectrometer facility (HRS) for pion detection and momentum analysis. The target system was a cryostat<sup>3</sup> which con-

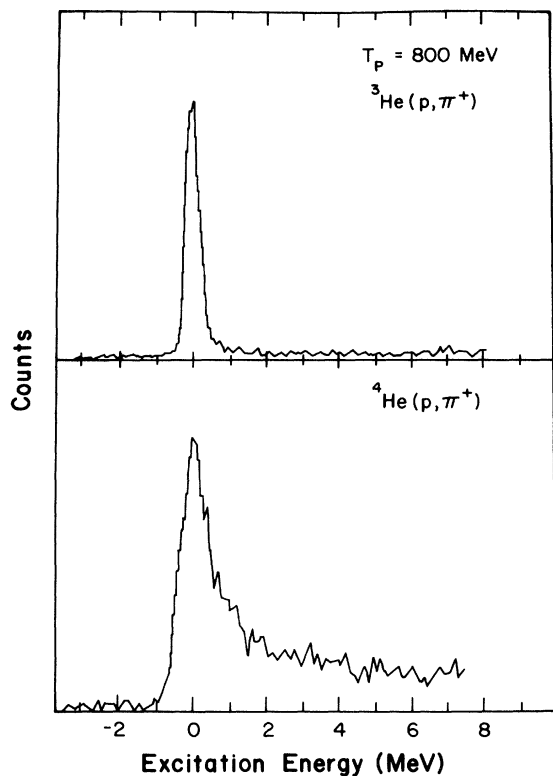


FIG. 1. Pion spectra from the  ${}^3,4\text{He}(p,\pi^+)$  reactions plotted as a function of excitation energy of the residual nuclei  ${}^4\text{He}$  and  ${}^5\text{He}$ , respectively.

tained liquid  ${}^3\text{He}$  and  ${}^4\text{He}$  in separate target cells, each of thickness  $\sim 0.75$  cm. The cryostat was constructed by a group at the University of Virginia, with the target cells modified at LAMPF in order to fit the HRS system. The pions were separated by the trigger system from the large number of inelastically scattered protons of the same momentum by differences in energy loss in one of the focal plane scintillation detectors, and by time of flight constraints from a 2 m flight path in the detector system near the focal plane of the HRS. The remaining background (probably positrons and electrons) was small, and could readily be subtracted from the pion peak in the spectra. Typical pion spectra from the  ${}^3,4\text{He}$  targets are shown in Fig. 1. The experimental energy resolution was typically 600 keV FWHM, with the main contribution coming from energy straggling in the target and its thermal shielding foils. This energy resolution is seen in the pion spectrum from  ${}^3\text{He}$ , while a much broader peak results from  ${}^4\text{He}$  owing to the intrinsic decay width of the  ${}^5\text{He}$  ground state. The errors in the data points for the  ${}^3\text{He}(p,\pi^+){}^4\text{He}$  reaction are mainly owing to statistics, and only a small contribution is attributed to uncertainties in the background subtraction. The extraction of the cross section for the  ${}^4\text{He}(p,\pi^+){}^5\text{He}$  reaction involves an empirical separation of pions leading to the broad  $1p_{1/2}$  excited state of  ${}^5\text{He}$ , as well as to the breakup of  ${}^5\text{He}$ . The error introduced by this separation process is included in the data points. In addition to the errors in the data points presented in this paper, there is an estimated  $\pm 15\%$  error

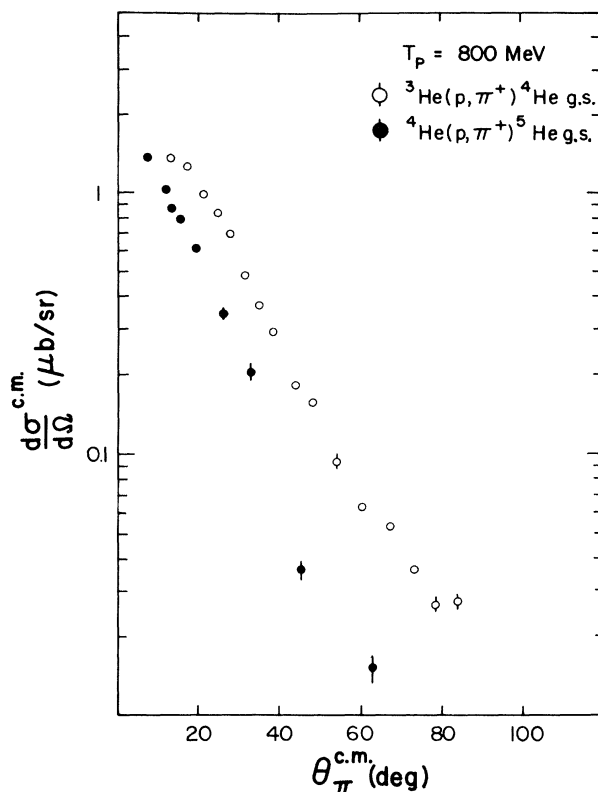


FIG. 2. Angular distributions of the differential cross section for the ground state transitions in the  ${}^3,4\text{He}(p,\pi^+){}^5\text{He}$  reactions at 800 MeV.

in the absolute cross section. The dominant contributions to this error are owing to the normalization of the data to the known  $pp \rightarrow d\pi$  reaction cross section,<sup>1</sup> and uncertainties in the target thickness and the trigger efficiency, including pion losses owing to nuclear reactions in the detectors.

### III. EXPERIMENTAL RESULTS

The angular distributions of the differential cross section for ground state transitions in the  ${}^3,4\text{He}(p,\pi^+){}^5\text{He}$  reactions are shown in Fig. 2. The distributions follow a rather featureless exponential slope, which is usually found for transitions in the  $1s-1p$  shell, regardless of incident energy. The  $(p,\pi^+)$  cross section on  ${}^4\text{He}$  appears from the figure to be slightly smaller than that from  ${}^3\text{He}$ . However, this only reflects the fact that a larger momentum transfer is involved in the pion production from  ${}^4\text{He}$ . When the two distributions are plotted versus momentum transfer the two data sets coincide, within the error bars. A few other features of the cross section data from  ${}^3\text{He}$  also appear more clearly from a presentation versus momentum transfer, as shown in Fig. 3. In the angular distribution a slight change in the slope is noticed at  $\sim 650$  MeV/c. For comparison, earlier data obtained at 716 MeV from Saclay<sup>4</sup> is included in the figure together with the charge form factor of  ${}^4\text{He}$  obtained from a fit to electron scattering.<sup>3</sup> We observe that the 716 MeV data also display a change in the slope at approximately the

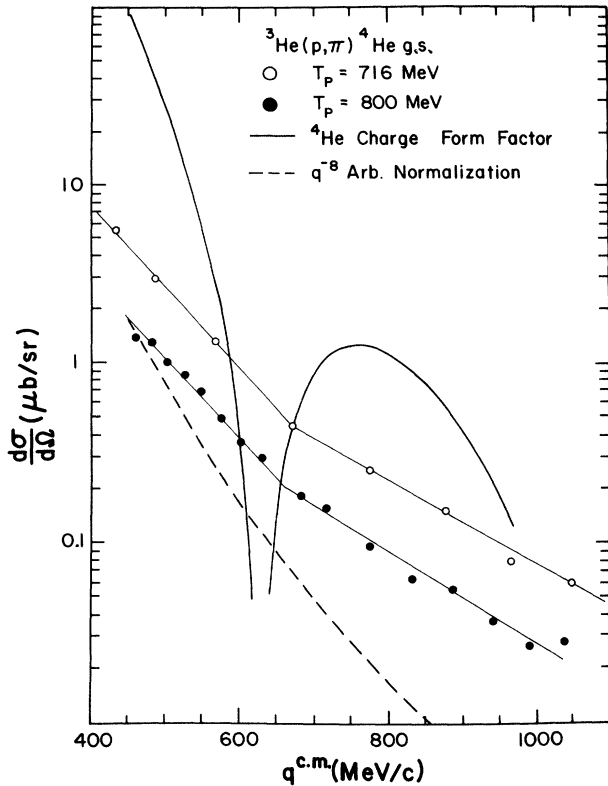


FIG. 3. Angular distributions of the differential cross section for the ground state transition in the  ${}^3\text{He}(p, \pi^+){}^4\text{He}$  reaction obtained at 716 (Ref. 3) and 800 MeV plotted versus total momentum transfer. The thin lines through the data points serve as a guide for the eye. The solid line represents the charge form factor of  ${}^4\text{He}$  obtained from electron scattering, and the dashed curve is a graph of the function  $q^{-8}$ . Both graphs are arbitrarily normalized.

same momentum transfer. We note that the charge form factor of  ${}^4\text{He}$  goes through a minimum close to this momentum transfer, but that could be just fortuitous. A more significant observation might be that the slope of the data for  $q \approx 400\text{--}600$  MeV/c is much less steep than the slope of the charge form factor in the same region of  $q$ . This may be an indication that momentum sharing is taking place in the reaction and that the slope of the angular distribution at large  $q$  is indeed determined by the form factor at some lower value of  $q$ . In fact, the data have the same slope as the form factor at  $\sim 250$  MeV/c.

From Fig. 3 it is also apparent that the  $(p, \pi^+)$  cross section decreases with increasing energy above the (33) resonance. This characteristic follows earlier observations from transitions in, for example, the  ${}^9\text{Be}(p, \pi^+){}^{10}\text{Be}$  reaction, for which data are available from threshold up to 800 MeV (see, for example, Ref. 5).

It should be pointed out that, although the angular distributions from the differential cross section seem to fall off exponentially with the momentum transfer  $q$ , one can equally well obtain a good fit to the data with a simple function  $q^{-n}$ . Such a behavior is, in fact, predicted in a model by Eisenberg,<sup>6</sup> who uses an eikonal approximation

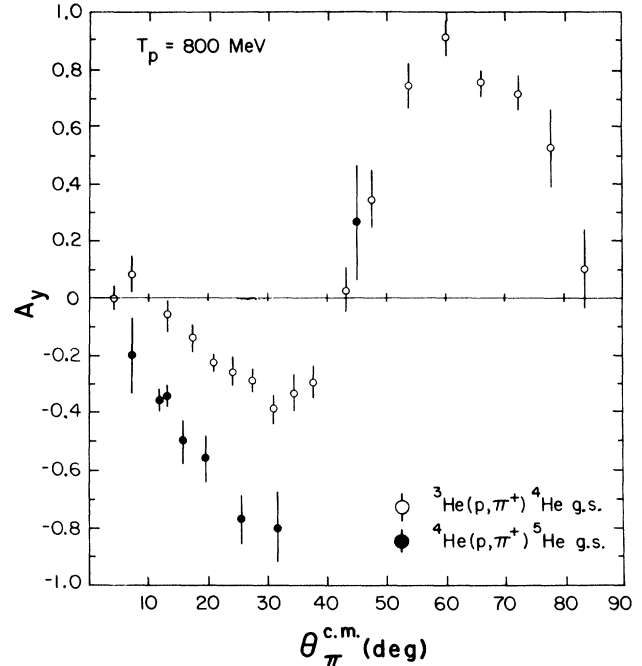


FIG. 4. Angular distributions of the analyzing power for the ground state transitions in the  ${}^3\text{He}(\vec{p}, \pi^+){}^4\text{He}$  reactions at 800 MeV.

in a DWBA calculation of the  $(p, \pi)$  cross section. In this model the differential cross section should fall as  $q^{-2L-8}$ , where  $L$  is the orbital angular momentum of the bound final state. Thus, a falloff of  $\sim q^{-8}$  is predicted for the  ${}^3\text{He}(p, \pi){}^4\text{He}_{\text{g.s.}}$  transition. This functional dependence is shown as the dashed curve in Fig. 3. The data, however, show a different picture. A good fit to the data is obtained with a function  $\sim q^{-5}$ , which is incompatible with the model mentioned above. However, in comparing the  ${}^3\text{He}(p, \pi){}^4\text{He}$  data with previous data at 800 MeV on the  ${}^9\text{Be}(p, \pi){}^{10}\text{Be}$  reaction,<sup>7</sup> we find the slope of the angular distribution of the  $(p, \pi)$  data from  ${}^9\text{Be}$  to be much steeper than that of the distribution from He. In fact, the distribution from Be falls like  $\sim q^{-12}$ , which might be easier to reconcile with the predicted  $q^{-10}$  dependence than the  $q^{-5}$  result for the  $(p, \pi)$  data on  ${}^3\text{He}$ .

The angular distributions of the analyzing power for the  ${}^3\text{He}(\vec{p}, \pi^+){}^4\text{He}_{\text{g.s.}}$  reactions are shown in Fig. 4. In contrast to the featureless slope of the differential cross sections, these analyzing power distributions show a remarkable angular dependence in the magnitude of the analyzing power  $A_y$ , which reveals a strong spin dependence in these reactions. A comparison could, for example, be made with data from the  $\vec{p}d \rightarrow t\pi$  reaction, which indeed show a similar shape in  $A_y$ , but with a magnitude no larger than 0.5 at all angles.<sup>2</sup> In the pion production from  ${}^3\text{He}$  and  ${}^4\text{He}$ , we note, in particular, the large difference in  $A_y$  at forward angles which in some sense must be attributed to nuclear structure differences. This feature could contain information about how details in the reaction process are dependent on the nuclear structure. Previous data on  $A_y$  from the He isotopes only exist at

threshold energies from  ${}^3\text{He}$ .<sup>8</sup> These data exhibit a negative  $A_y$  at all angles with a minimum value of  $-0.7$  close to  $90^\circ$ .

#### IV. DISCUSSION OF THE DATA IN TERMS OF SUBPROCESSES IN THE $(p, \pi)$ REACTION

The data from the  ${}^3,4\text{He}(\bar{p}, \pi^+){}^4,5\text{He}$  reactions do not invite any obvious speculation about the reaction mechanism. The features of the data are not easily recognized as a sign of any particular dynamic process. However, one should perhaps not expect any immediate answer from the He data, since we have only a vague understanding of the dynamics involved for pion production in the elementary  $pp \rightarrow d\pi$  reaction at and above 800 MeV,<sup>9,15</sup> not to mention the interpretational difficulties of the  $(p, \pi)$  reaction on nuclei at all energies.

As a first crude analysis of the present  $(\bar{p}, \pi)$  data on He we would like to investigate to what extent these data show similarities with other simpler processes which could be plausible subprocesses in the  $(p, \pi)$  reaction. For example, the analyzing power might show some resemblance to  $A_y$  from elastic proton scattering if proton distortion (the spin-orbit interaction) is important. Another possibility would be to trace features of the  $\bar{p}p \rightarrow d\pi$  reaction in the present data, which could be found if this reaction plays the role of a subprocess in the  $(\bar{p}, \pi^+)$  reaction on He. If pion rescattering is a crucial ingredient in the reaction dynamics, this might lead to some similarities with data from elastic pion-nucleon scattering. In the following, data from these three subprocesses are compared with the analyzing power from the  ${}^3\text{He}(\bar{p}, \pi^+){}^4\text{He}$  reaction under specific assumptions about the momentum sharing in the  $(p, \pi)$  reaction.

##### A. Comparison with elastic proton scattering on He

As a first case we compare the analyzing power data from elastic proton scattering at 800 MeV on  ${}^3\text{He}$  (see Ref. 10) and  ${}^4\text{He}$  (see Ref. 11) with the corresponding  $(p, \pi)$  data. This is done simply by plotting these data versus c.m. angle as shown in Fig. 5. Since only a very qualitative comparison is attempted, only a curve through the  $(p, p)$  data is shown. From this figure it is seen that the sharp minimum in the angular distribution of  $A_y$  from elastic  $(p, p)$  scattering on He indeed coincides approximately with the minimum at  $\sim 35^\circ$  in  $A_y$  from  $(p, \pi)$ . However, both the magnitude and the detailed shape of the distributions differ substantially. Moreover, the relative difference between the  $A_y$  distributions from  $(p, p)$  on  ${}^3\text{He}$  and  ${}^4\text{He}$  does not show up in any similar way for the  $A_y$   $(p, \pi)$  data on the same nuclei. The deeper minimum in  $A_y$  from  $(p, \pi)$  on  ${}^4\text{He}$  has no counterpart in the He $(p, p)$   $A_y$  data. One might expect that to first order the  $A_y$  data for  $(p, p)$  and  $(p, \pi)$  on nuclei should qualitatively behave the same, if the spin-orbit distortion is the driving force which generates the analyzing power in the  $(p, \pi)$  reaction. Since very few similarities exist in the  $A_y$  data from  $(p, p)$  and  $(p, \pi)$  on He, we find no evidence that the analyzing power in the  $(p, \pi)$  reaction should be attributed to proton

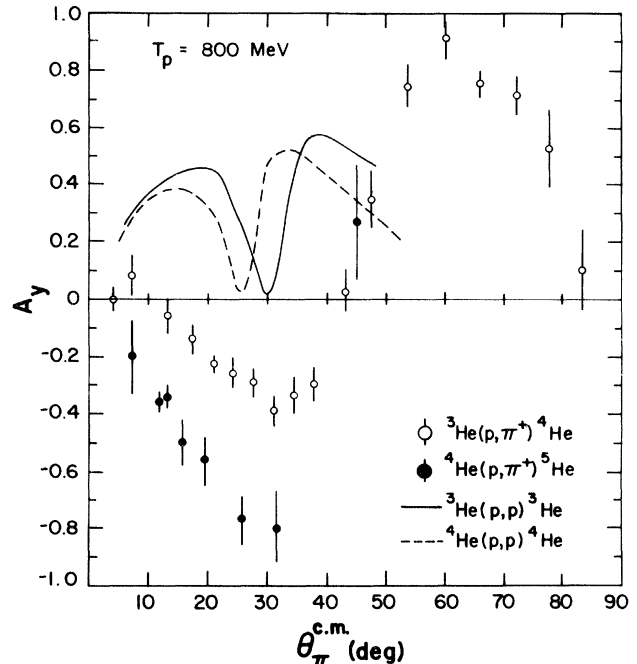


FIG. 5. A comparison between the angular distributions of the analyzing powers for the  $(\bar{p}, \pi^+)$  reaction and elastic proton scattering on  ${}^3\text{He}$  and  ${}^4\text{He}$  obtained at 800 MeV. The solid and dashed curves represent the data for the elastic proton scattering from  ${}^3\text{He}$  and  ${}^4\text{He}$ , respectively.

distortion. Of course general proton and pion distortion could indirectly be an important factor in determining  $A_y$  in  $(p, \pi)$  by localizing the reaction to certain parts of the nucleus, which might disguise the pure features of the mechanism which produces the asymmetry in the  $(p, \pi)$  reaction.

It should be pointed out that a different comparison of data from elastic scattering and nuclear reactions has been suggested by Shepard and Rost,<sup>14</sup> who from an analytic approach to the DWBA approximation find it more justified to compare the different data sets as a function of transverse momentum transfer  $q_\perp$ . However, when this is done for the data presented in Fig. 5, no significant changes occur, and the same differences prevail. In this context we should mention that when the method of presenting data vs  $q_\perp$  is employed, we find that the low energy ( $T_p = 198$  MeV)  $A_y$  data<sup>8</sup> for the  ${}^3\text{He}(\bar{p}, \pi^+){}^4\text{He}$  reaction in fact coincide with the 800 MeV  $A_y$  data, except for some discrepancy in the magnitude of  $A_y$ . This is not the case if these two data sets are plotted vs  $\theta_{\text{lab}}$ ,  $\theta_{\text{c.m.}}$  or total momentum transfer.

##### B. Comparison with the $pp \rightarrow d\pi$ reaction

In a second trial case to find a subprocess in the  $(p, \pi)$  reaction we now consider the  $pp \rightarrow d\pi$  reaction. Several attempts to describe the  $(p, \pi)$  reaction phenomenologically in terms of the  $pp \rightarrow d\pi$  cross section have been made in the past for light nuclei. These works, reviewed by Fearing in Ref. 12, consider only the differential cross section

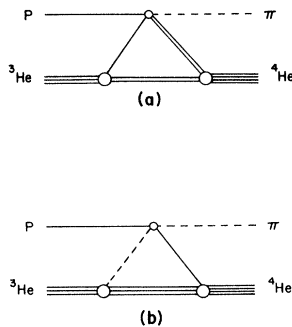


FIG. 6. (a) Diagram of the  ${}^3\text{He}(p,\pi){}^4\text{He}$  reaction showing the  $\text{NN}\rightarrow\text{NN}\pi$  reaction as a subprocess. (b) Diagram of the  ${}^3\text{He}(p,\pi){}^4\text{He}$  reaction containing pion emission from the target and rescattering via the incident proton.

at energies up to 600 MeV. We are interested in knowing how the new data on the analyzing power in the  $(\bar{p},\pi)$  reaction from  ${}^3\text{He}$  compare with  $A_y$  data from  $\bar{p}p\rightarrow d\pi$ . A remark should first be made as to why the  $pp\rightarrow d\pi$  reaction is considered rather than the three-body reactions  $pp\rightarrow np\pi$  or  $pn\rightarrow nn\pi$ , which also lead to positive pion production. For this purpose a diagram of the  ${}^3\text{He}(p,\pi){}^4\text{He}$  reaction, showing the  $\text{NN}\rightarrow\text{NN}\pi$  subprocess explicitly, is given in Fig. 6(a). Conservation of isospin can be applied to the three different vertices in this triangle diagram. Comparing the  $pp\rightarrow d\pi$  and the  $pn\rightarrow nn\pi$  reactions occurring in the upper vertex, we find that the former is twice as likely when the assumption is made that the intermediate state is a  $T=1, \Delta N$  state. With  ${}^3\text{He}$  as target, there are twice as many  $pp$  collisions as  $pn$  collisions, which gives another factor of 2 in favor of  $pp\rightarrow d\pi$ . The  $pp\rightarrow d\pi$  reaction should thus dominate by a factor of 4 over the  $pn\rightarrow nn\pi$  reaction. Regarding the relative importance of the  $pp\rightarrow d\pi$  and  $pp\rightarrow np\pi$  reactions, this is a matter of knowing by how much the formation of the bound  $T=0, S=1$   $np$  pair dominates over the unbound  $T=1, S=0$   $np$  pair. Observe that only relative  $s$  states are considered since the  $np$  pair should be bound to  ${}^4\text{He}$ . Using isospin in the upper vertex, we find that the formation of the  $T=0$   $np$  pair is twice as likely as the formation of the  $T=1$   $np$  pair. In the lower left vertex one gets that the  $T=0$   $np$  pair in  ${}^3\text{He}$  is three times more frequent than the  $T=1$   $np$  pair. Finally, in the lower right vertex, the formation of  ${}^4\text{He}$  from two  $T=0$   $np$  pairs is three times more probable than from two  $T=1$   $np$  pairs. Consequently, the  $pp\rightarrow d\pi$  reaction, which has the  $np$  pair in a  $T=0$  state, should dominate by a total factor of 18 over the  $pp\rightarrow np\pi$  reaction, when these reactions are considered as subprocesses in the  ${}^3\text{He}(p,\pi){}^4\text{He}$  reaction. Considering the isospin conservation only, we can then conclude that the  $pp\rightarrow d\pi$  reaction should be the dominant subprocess in a reaction picture described by Fig. 6(a).

It should be remarked that at 800 MeV the free  $pp\rightarrow np\pi$  total cross section is about ten times larger than the free  $pp\rightarrow d\pi$  total cross section, which might be used as an argument against using the  $pp\rightarrow d\pi$  amplitude exclusively in our comparison with the  $(p,\pi)$  reaction. However, the bigger cross section for the  $pp\rightarrow np\pi$  reaction is

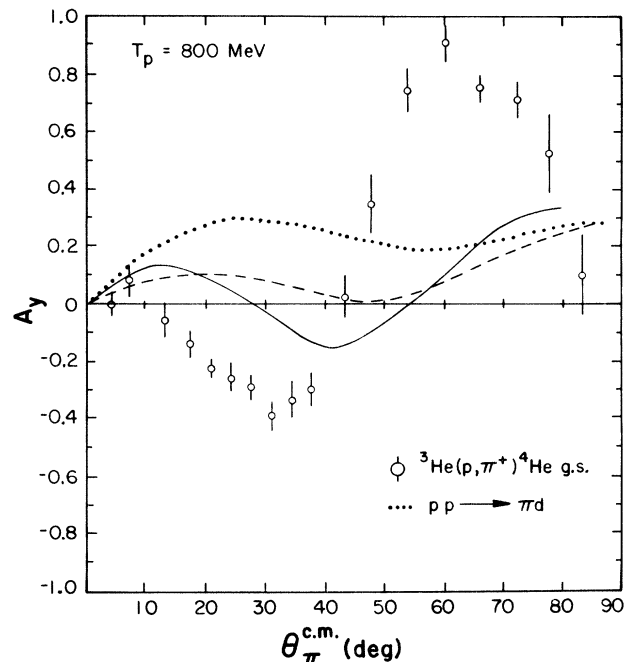


FIG. 7. Comparison between the angular distributions of the analyzing powers for the  ${}^3\text{He}(\bar{p},\pi){}^4\text{He}$  and the  $\bar{p}p\rightarrow d\pi$  reactions based on different assumptions about momentum sharing. The dotted line is a fit to the  $\bar{p}p\rightarrow d\pi$  data at 800 MeV. The dashed and solid lines represent the  $\bar{p}p\rightarrow d\pi$  data at different energies as explained in the text.

mainly owing to the larger phase space, which is available for the three-body final state. Using the  $pp\rightarrow np\pi$  reaction as a subprocess in the  ${}^3\text{He}(p,\pi){}^4\text{He}$  reaction, this phase space is reduced considerably, since the captured neutron and proton must have momentum components determined by the  ${}^4\text{He}$  form factor. In fact, the situation when the two nucleons move together is favored, because the momentum sharing is then optimized in the  $(p,\pi)$  reaction. It is therefore not likely that the cross sections for  $pp\rightarrow np\pi$  and  $pp\rightarrow d\pi$  reactions differ very much when confined to the phase space available in the  ${}^3\text{He}(p,\pi){}^4\text{He}$  reaction. The same arguments can be applied to the  $pn\rightarrow nn\pi$  reaction, although in this case the phase space restrictions are of less importance, since the  $pn\rightarrow nn\pi$  total cross section is only about a factor of 2 larger than that of  $pp\rightarrow d\pi$ . The conclusions based on isospin favoring the  $pp\rightarrow d\pi$  subprocess are thus the dominating selection criteria.

A comparison between  $A_y$  from the  $\bar{p}p\rightarrow d\pi$  and the  ${}^3\text{He}(\bar{p},\pi){}^4\text{He}$  reactions can be made in different ways. The easiest way is simply to compare the two data sets at the same laboratory energy, and present the angular distributions in the same Lorentz frame. In Fig. 7 the  $pp\rightarrow d\pi$  analyzing power at 800 MeV (Ref. 9) is presented in the  ${}^3\text{He}$  c.m. system together with the  $A_y$  data from the  ${}^3\text{He}(p,\pi){}^4\text{He}$  reaction. For convenience, only a dotted curve through the  $pp\rightarrow d\pi$  data is shown. From this figure it is hard to see any connection between these two reactions. The differences are surprisingly large. This sug-

gests that the dynamics in the pion production in the  $pp \rightarrow d\pi$  reaction is very different from that in  $(p,\pi)$  on  ${}^3\text{He}$ , which is not easy to accept. It is therefore relevant to question whether this type of comparison, i.e., at the same laboratory energy, is justified at all. The physical picture behind this comparison is that the incident proton collides with a stationary target proton (provided it is on the mass shell), that is, this proton has zero momentum relative to the center of mass of the target nucleus. Consequently, the large momentum transfer involved in the  ${}^3\text{He}(p,\pi){}^4\text{He}$  reaction ( $q_{\text{c.m.}} = 432 \text{ MeV}/c$  at  $0^\circ$  and  $1088 \text{ MeV}/c$  at  $90^\circ$ ) has to occur when the deuteron is captured by the residual nucleus, and no momentum sharing is taking place. One might argue that this is not a very favorable way to transfer a large momentum to the residual nucleus. A more preferred way would be to have momentum sharing between the nuclear vertices, that is, the two lower vertices in Fig. 6(a). We therefore examine the case in which a specific sharing of the total momentum transfer between the lower left and right vertex is assumed. Two somewhat arbitrarily chosen cases are investigated, namely, when  $|\bar{q}_L| = |\bar{q}_R|$  and when  $|\bar{q}_L| = \frac{1}{2} |\bar{q}_R|$ , where  $\bar{q}_L$  and  $\bar{q}_R$  are the momentum transfers involved in the left and right lower vertices in the diagram of Fig. 6(a), respectively. Assuming momentum conservation in each vertex, this imposed constraint about the momentum sharing determines the momentum of the target proton before the collision. The direction of the momentum of the target proton is assumed to be parallel and towards the momentum of the incident proton, since this configuration minimizes the necessary momentum transfer in each vertex. It is now a straightforward task to calculate the momentum of the target proton before the collision for each scattering angle of the outgoing pion. In the angular region  $\theta_\pi$  c.m. =  $0^\circ - 80^\circ$  the proton momentum varies between 440 and 542 MeV/c when  $|\bar{q}_L| = \frac{1}{2} |\bar{q}_R|$ , and between 506 and 670 MeV/c when  $|\bar{q}_L| = |\bar{q}_R|$ . The momenta are given in the  $p^3\text{He}$  c.m. system. In this reaction picture the incident proton hits a target proton which is moving towards it. Consequently, the energy at which the  $pp \rightarrow d\pi$  reaction should be compared with the  ${}^3\text{He}(p,\pi){}^4\text{He}$  reaction is dependent on the magnitude of the target proton's momentum. Since this momentum varies with scattering angle, the energy to be used for the  $pp \rightarrow d\pi$  reaction,  $T_{pp \rightarrow d\pi}$ , changes accordingly. In calculating these energies we have assumed that the target proton is on its mass shell. This implies that the captured deuteron has to be slightly off shell, and the use of on shell  $pp \rightarrow d\pi$  data is an approximation. In the angular region  $0^\circ - 80^\circ$   $T_{pp \rightarrow d\pi}$  varies in the laboratory system between 953 and 1159 MeV when  $|\bar{q}_L| = \frac{1}{2} |\bar{q}_R|$  and between 1096 and 1388 MeV when  $|\bar{q}_L| = |\bar{q}_R|$ . Unfortunately, our experimental knowledge about the analyzing power of the  $pp \rightarrow d\pi$  reaction in this energy region is not very satisfactory. Good data exist up to 1 GeV from Saclay,<sup>15</sup> and another measurement at 1234 MeV has been reported from Argonne.<sup>16</sup> Although the energy variation in the  $pp \rightarrow d\pi$  data is significant, the general trend of the data at the energies needed for our purpose can be obtained by interpolation. Using this experimental information, the analyz-

ing power from the  $pp \rightarrow d\pi$  vertex can now be obtained. The calculation is done with respect to the  $p^3\text{He}$  c.m. system, for the two cases of momentum sharing given above, and the result is presented in Fig. 7. We note with interest that this approach leads to a better similarity between the  $\bar{p}p \rightarrow d\pi$  and  ${}^3\text{He}(\bar{p},\pi){}^4\text{He}$  data than was found when no momentum sharing was required. In fact, one can no longer rule out that the production process in the  $pp \rightarrow d\pi$  reaction is a part of the process also in the  ${}^3\text{He}(p,\pi){}^4\text{He}$  reaction. It should be remembered, though, that the use of extrapolated information from the existing  $pp \rightarrow d\pi$  data implies that the curves in Fig. 7 should be seen as general trends rather than absolute predictions. It should also be emphasized that the energies  $T_{pp \rightarrow d\pi}$  are calculated under the assumption that the target proton is on the mass shell. If this condition is relaxed and the proton as well as the deuteron is allowed to go far off shell differently for each scattering angle, then  $T_{pp \rightarrow d\pi}$  will have different values. However, with the  $pp \rightarrow d\pi$  reaction being far off shell, it is not very meaningful to make the comparison with on shell  $pp \rightarrow d\pi$  data. For the sake of completeness, the case when the deuteron is on its mass shell, instead of the proton, has also been investigated. The results from this calculation do not differ qualitatively from those presented in Fig. 7.

### C. Comparison with the pion-nucleon scattering

As a third way to analyze the  ${}^3\text{He}(\bar{p},\pi){}^4\text{He}$  data we chose to investigate the extent to which the analyzing power from elementary pion-nucleon scattering,  $\pi\vec{N}$ , is reflected in the data. Such a comparison is motivated in a reaction picture where pion rescattering is part of the reaction dynamics. This can happen in two ways. Either the incident proton emits a pion (projectile emission) which is then rescattered on a target nucleon, or a pion is emitted from the target nucleus (target emission), in which case the pion is rescattered on the incident projectile. The last process can be considered as a knockout of a virtual pion in the nucleus. We investigate this case because it leads to a direct comparison with  $\pi\vec{N}$  data. The target emission process has been applied by Gibbs<sup>13</sup> in microscopic calculations of certain nuclear transitions at threshold energies. Our objective is to use the same model, but at a much less sophisticated level, by making merely a phenomenological comparison with  $\pi\vec{N}$  data. For the projectile emission diagram the situation is more involved and it is not so obvious how to link the  $\pi\vec{N}$  data into the  $(\bar{p},\pi)$  process.

The diagram for the target emission is shown in Fig. 6(b). As in the  $pp \rightarrow d\pi$  case, we now have to determine at what energy the  $\pi\vec{N}$  data should be compared with the  ${}^3\text{He}(p,\pi){}^4\text{He}$  data. Our first approach is to consider the outgoing channel where a real pion is emitted. The  ${}^3\text{He}(p,\pi){}^4\text{He}$  reaction at 800 MeV is identical to the reversed reaction  ${}^4\text{He}(\pi,p){}^3\text{He}$  taking place at 480 MeV. We use  $\pi\vec{N}$  data at this fixed pion energy to describe the upper vertex in the figure. This is consistent with a picture in which an 800 MeV incident proton collides with an

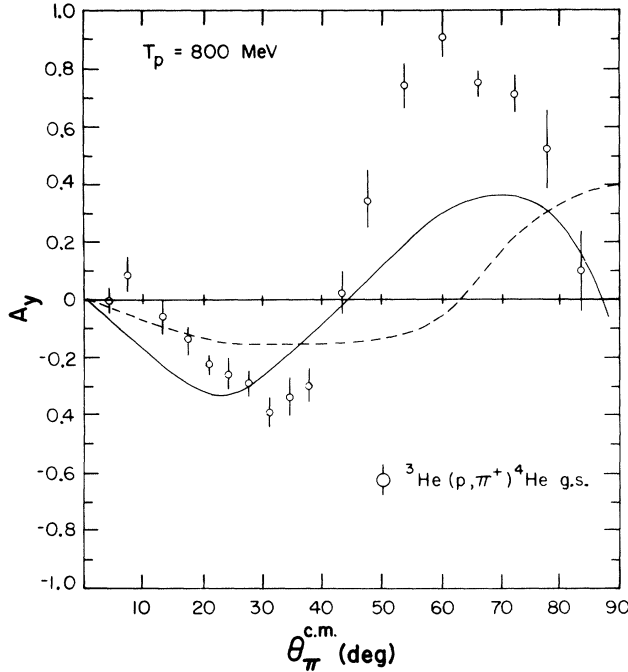


FIG. 8. Comparison between the angular distribution of the analyzing powers for the  ${}^3\text{He}(\vec{p}, \pi^+) {}^4\text{He}$  reaction and the elastic pion-nucleon scattering, based on different assumptions about momentum sharing. The dashed line represents the  $\pi\vec{p}$  data at 480 MeV and the solid line represents the  $\pi\vec{p}$  data from different energies as explained in the text.

off-shell pion in the target nucleus, leading to emission of a real pion and capture of an on-shell proton to the target nucleus. Moreover, it can be shown that the total momentum transferred to the nucleus takes place in the lower left pion emission vertex only, with zero momentum being transferred in the proton capture vertex. The situation is similar to the one in which the  $pp \rightarrow d\pi$  reaction was taken at a fixed energy, with the consequence that no momentum sharing would take place.

A positive pion can appear in the final state when the upper vertex in Fig. 6(b) represents either elastic  $\pi^+p \rightarrow \pi^+p$  scattering or the charge exchange  $\pi^0p \rightarrow \pi^+n$  reaction. Consequently, both these processes have to be considered in the comparison with the  $(p, \pi)$  data. It should also be remarked that pion production at  $0^\circ$  corresponds to  $\pi\vec{N}$  scattering at  $180^\circ$ , since we consider the subprocess as a pion "knockout." Using available polarization data from elastic scattering as well as from charge exchange at 480 MeV,<sup>17</sup> complemented with information from a global phase shift analysis,<sup>17</sup> and transforming these data to the  ${}^3\text{He}$  c.m. system, we get the result shown in Fig. 8. Since our intention is merely to look for traces of a  $\pi N$  subprocess, and since the individual contributions from the  $\pi^+p \rightarrow \pi^+p$  and  $\pi^0p \rightarrow \pi^+n$  reaction do not differ substantially, we simply show the average result, represented as a dashed line in Fig. 8. The resemblance between this curve and the  ${}^3\text{He}(\vec{p}, \pi^+) {}^4\text{He}$   $A_y$  data is not overwhelming. No conclusion about the relevance of the  $\pi\vec{N}$  rescattering seems to be justified from this com-

parison. However, as pointed out above, this approach does not involve momentum sharing between the pion emission vertex and the nucleon capture vertex. It would therefore be interesting to investigate the case when momentum sharing takes place. Let us assume that an equal momentum is transferred at the two lower vertices in Fig. 6(b) ( $|\vec{q}_L| = |\vec{q}_R|$ ). We also keep the condition that the captured nucleon should be on its mass shell, since it is easier for the pion to go off shell than for the nucleon to do so. The initial momentum of the pion emitted by the target nucleus as well as the equivalent angle dependent laboratory energy  $T_{\pi N}$  for the pion nucleon scattering can now be calculated. In the  $(p, \pi)$  angular range  $0^\circ - 80^\circ$ , the pion momentum varies between 303 and 553 MeV/c ( ${}^3\text{He}$  c.m. system), and  $T_{\pi N}$  varies between 334 and 755 MeV. Following the same procedure outlined above for the  $pp \rightarrow d\pi$  reaction, we get the solid curve presented in Fig. 8. This curve should only be regarded as qualitative since the available  $\pi\vec{N}$  data are not very accurate at all energies in the interval considered. It is interesting to note that the general shape of the curve follows the  $(p, \pi)$  data, although the magnitude of  $A_y$  is too small. As in the comparison with the  $pp \rightarrow d\pi$  reaction, introducing momentum sharing between the nuclear vertices improves the fit to the data. We also observe that the result from the  $pp \rightarrow d\pi$  and  $\pi N$  approaches are not too different. This is perhaps not so surprising, since pion rescattering is part of the  $pp \rightarrow d\pi$  amplitude, and thus there will be a certain amount of overlap between the two approaches. The moderate success obtained by using the  $\pi N$  subamplitude suggests that the analyzing power in the  $(p, \pi)$  reactions is largely caused by pion rescattering.

## V. SUMMARY AND FINAL REMARKS

Angular distributions for the differential cross sections and the analyzing power from the  ${}^3, {}^4\text{He}(\vec{p}, \pi^+) {}^4, {}^5\text{He}_{g.s.}$  reactions at 800 MeV have been presented. The differential cross section data were compared with the charge form factor of  ${}^4\text{He}$ , which showed that the  $(p, \pi)$  distribution has a less steep slope than the form factor in the same range of momentum transfer, thereby suggesting that momentum sharing is taking place. The angular distribution for the analyzing power of the  ${}^3\text{He}(\vec{p}, \pi^+) {}^4\text{He}$  reaction was compared with corresponding data from elastic proton scattering, the  $pp \rightarrow d\pi$  reaction, and pion nucleon scattering, in order to investigate whether any of these processes could play a role in the  $(p, \pi)$  reaction. No similarities with elastic proton scattering on He were found which could be used as evidence for proton distortion being a significant source in creating asymmetries in the  $(p, \pi)$  reaction. Comparison with the analyzing power data for the  $\vec{p}p \rightarrow \pi d$  reaction showed some similarities with the  $(\vec{p}, \pi)$  data, and the comparison with the  $\pi\vec{N}$  scattering data gave even better agreement, provided that equal momentum sharing was imposed between the nuclear vertices. This result suggests that pion rescattering and momentum sharing are important ingredients in the  $(p, \pi)$  reaction. This might have been expected, but it is perhaps surprising that the on-shell subprocesses can, in fact, be utilized with some success. A noticeable

discrepancy between the  $(p,\pi)$  data and the predictions from the  $pp \rightarrow \pi d$  or  $\pi N$  amplitudes is the difference in the magnitude of  $A_y$ . This fact might be attributed to the specific constraint imposed by the nuclear transitions involved, and does not necessarily rule out a relation to these subprocesses. Moreover, an interplay between the reaction mechanism and the nuclear structure could certainly prevail, which makes a direct connection to the elementary on shell processes obscure. Of course, only a comprehensive theoretical model calculation can lead to a quantitative conclusion about the details in the reaction

dynamics. In particular, the role of the nuclear structure, as manifested for example by the difference in  $A_y$  from the  ${}^3\text{He}$  and  ${}^4\text{He}$  target nuclei, needs to be explained.

#### ACKNOWLEDGMENTS

Many stimulating and valuable discussions with W. R. Gibbs and J. M. Eisenberg are gratefully acknowledged. This work was supported by the U.S. Department of Energy.

---

<sup>1</sup>A recent comprehensive review of this field is given in *Pion Production and Absorption in Nuclei—1981 (Indiana University Cyclotron Facility)*, Proceedings of the Conference on Pion Production and Absorption in Nuclei, AIP Conf. Proc. No. 79, edited by Robert D. Bent (AIP, New York, 1982).

<sup>2</sup>K. K. Seth *et al.*, Northwestern University Annual Progress Report 1981–82; D. Kielczewska *et al.*, International Conference on Few-Body Problems in Physics, Karlsruhe, 1983.

<sup>3</sup>J. S. McCarthy, I. Sick, and R. R. Whitney, Phys. Rev. C **15**, 1396 (1977).

<sup>4</sup>B. Tatischeff *et al.*, Phys. Lett. **63B**, 158 (1976).

<sup>5</sup>B. Höistad, see Ref. 1, p. 122.

<sup>6</sup>J. M. Eisenberg, see Ref. 1, p. 3.

<sup>7</sup>B. Höistad *et al.*, Phys. Rev. Lett. **43**, 487 (1979).

<sup>8</sup>J. J. Kehayias *et al.*, Indiana University Cyclotron Facility An-

nual Report, 1981.

<sup>9</sup>K. K. Seth *et al.*, Phys. Lett. **126B**, 164 (1983).

<sup>10</sup>A. Azizi (private communication).

<sup>11</sup>H. Courant *et al.*, Phys. Rev. C **19**, 104 (1979).

<sup>12</sup>H. W. Fearing, in *Progress in Particle and Nuclear Physics*, edited by D. H. Wilkinson (Pergamon, London, 1981), Vol. 7, p. 113.

<sup>13</sup>W. R. Gibbs, see Ref. 1, p. 297.

<sup>14</sup>J. R. Shepard and E. Rost, Phys. Rev. C **25**, 2660 (1982).

<sup>15</sup>R. Bertini *et al.*, Saclay report DPH-N/82.9.2., 1982.

<sup>16</sup>M. D. Corcoran *et al.*, Phys. Lett. **120B**, 309 (1983).

<sup>17</sup>D. Fitzgerald (private communication); G. Bizard *et al.*, Nucl. Phys. **B5**, 515 (1968); J. F. Martin *et al.*, *ibid.* **B89**, 253 (1975); R. M. Brown *et al.*, *ibid.* **B144**, 287 (1978); R. A. Arndt and L. D. Roper, VPI phase shift code.